Design and Experimental Evaluation of the Flywheel System for Power Leveling

*Jun-ichi Itoh, *Kenta Tanaka, *Yuji Saiki, *Noboru Yamada, **Koji Kato
*Nagaoka University of Technology
Nagaoka, Japan
itoh@vos.nagaokaut.ac.jp
** Sanken Electric Co., Ltd.
Saitama, Japan
k.kato@sanken-ele.co.jp

Abstract— **This paper introduces the performance of a power leveling system with a 3.0-MJ, 3315-r/min flywheel energy storage. In terms of cost reduction, this system uses low cost ball bearings and general purpose induction motor. Therefore, such a system configurations occurs large loss during standby mode. In order to overcome this problem, low loss design algorithm that focuses on the mechanical loss is applied to the design of the flywheel. As a result, the flywheel loss in the steady state consists of bearing loss of 28.3%, the copper loss of 22.5% for the induction motor. Moreover, charging and discharging efficiency are measured to evaluate the prototype flywheel system. From the analysis, it is confirmed that the charging efficiency is 75.4% and the discharging efficiency is 77.2%.**

Keywords—Flywheel, Low loss design, Loss analysis

I. INTRODUCTION

Renewable energy systems, especially a wind turbine and a photovoltaic cell, generated a power fluctuation due to the meteorological conditions. Therefore, these systems require energy buffers such as electric double layer capacitors (EDLC), batteries or flywheels to suppress the power fluctuations. For example, the battery can achieve a high energy density at low cost. However, one of the problems in the battery energy storage is a short life time. In particular, the lifetime depends on an ambient and the number of charge and discharge time. In addition, the battery cannot cope with rapid charge and discharge by a large internal resistance of the battery. On the other hand, the EDLC has a high charge and discharge efficiency. Moreover, the rapid charge and discharge is possible because the internal resistance is very small. However, similar to the battery, the lifetime is decreased rapidly due to the influence of the ambient temperature [1]. On the other hand, the flywheels has some advantages: (i) environmental friendly, (ii) low maintenance cost, (iii) long lifetime due to no chemical structure, and (iv) the charge and discharge characteristic of high cycle are excellent. For these reason, the flywheel has attracted attention as an energy storage system.

In recent years, an ultra-high speed rotation of the flywheel has been studied. The kinetic energy which is stored in the flywheel is proportional to the square of the rotational speed. Therefore, the magnetic bearings have been studied in order to achieve high energy density. However, the magnetic bearing is required an additional control system [2-4]. For this reason, it can lead to high cost and complexity of the control system of the flywheel system.

Therefore, it is necessary to achieve the flywheel systems that do not use a magnetic bearing. The authors have evaluated a prototype flywheel consists of the induction machine with ball bearings [5][6]. From the loss analysis of the prototype flywheel system, it is confirmed that the steady state loss of the flywheel is very large. Therefore, it is necessary to establish a method for low loss design of the flywheel and the further loss reduction toward the practical use of the flywheel.

In this paper, the design method of the flywheel which aims to reduce the mechanical loss is established. This approach focuses on the design freedom of the shape of the flywheel to store the same energy. The constitution of this paper is follows: at first, the proposed flywheel system is introduced. Next, the design method of the flywheel shape is discussed. Thirdly, the analytical technique of the loss that occurs in the flywheel is investigated. Finally, the steady state loss and the energy stored efficiency are evaluated by the experiments.

II. PROPOSED FLYWHEEL SYSTEM

Fig. 1 shows the configuration of a proposed flywheel system that employs the general purpose motor and ball bearings. In this system, it is possible to store the kinetic energy of the 3.0 MJ at 3315 r/min. Such a low rotation speed region can be applied to a typical ball bearing and general purpose motor. In addition, the flywheel vacuum case and the motor are separated by the magnetic fluid seal. As a result, windage loss can be greatly reduced because it is possible to reduce a pressure in the vacuum case by the vacuum pump. Moreover, vacuum in the vacuum case does not affect the heat dissipation of the motor because the motor and the vacuum case are separated. Therefore, the general purpose motor can be applied to drive the flywheel without adding special cooling mechanism.

Fig. 2 shows the block diagram of the flywheel system including the measurement system and auxiliary devices. In the flywheel system, the induction machine is operated as a generator during deceleration, the kinetic energy is converted into the electrical energy. On the other hand, during acceleration, the electrical energy is stored as the kinetic energy, which is working as a motor. Therefore, this system uses a regenerative converter. Furthermore, an over temperature of the bearing and the motor can be prevented by the oil cooler.

III. Low Loss Design of the Flywheel Shape

A. Consideration of the basic model

Fig. 3 shows the low loss design flow of the flywheel [7]. In this design approach, it is necessary to consider the basic model such as the direction of the rotation of the flywheel and the bearing types. The rotational direction of the flywheel can be considered vertical and horizontal. In the vertical axis, the horizontal axis is not bent because the load of the flywheel will be loaded in the axial direction. Therefore, the effects of the shaft whirling will be excluded from the design items. In the bearing loss, the effect of the rotational speed is larger than the influence of the load.

In this study, the flywheel is designed to give priority to a loss reduction and a safety. Therefore, the vertical axis is chosen as the rotational direction of the flywheel.

B. Setting the required specifications

In this process, the specification of the flywheel which is required for the system is considered. The design items to be set are follows: the maximum dimension, the maximum rotation speed, the stored energy of the flywheel, performances of the safety and the lifetime. The shape of the flywheel satisfying these conditions is enormous. Therefore, the shape of the flywheel is designed automatically by the low loss design algorithm.

The required specifications of the prototype flywheel are as follows: the maximum radius of the flywheel is 0.5 m, the maximum thickness is 0.5 m, the maximum rotation speed is 10000 r/min, the bearing life is 10 years. These specifications assume a size that can be processed by a machine tool or a production company in general.

C. Determination of the specification

In this process, the combination of the design parameters that satisfy the required specification are determined. For example, the windage loss varies greatly depending on the ratio of the radius of the vacuum case and the flywheel. Therefore, the design parameters such as the radius and speed of the flywheel vary from a minimum value to a maximum value. As a result, a variety of specifications of the flywheel to meet the required value is determined.

D. Evaluation of the mechanical loss

In this process, the bearing loss and the windage loss are calculated for a provisional specification was determined. Note that the bearing loss and the windage loss are calculated by the analytical method which is described in the next section. In addition, the windage loss and the bearing loss calculated in this process are compared to the mechanical loss obtained in different specifications. Finally, the specification of the flywheel which minimizes the mechanical loss is determined.

Table 1 shows the specification of the flywheel which is designed by the low loss design algorithm. From the results, it can be seen that the shape of the flywheel is disk-shaped. It is capable of storing sufficient energy for a low rotational speed by the inertia weight is increased. In addition, the windage loss and the bearing losses are reduced by the reduction in rotational speed. The pressure in a vacuum case is reduced by using a vacuum pump prior to operation in order to reduce the windage loss. In addition, the magnetic fluid seal is adopted to maintain the vacuum in the vacuum case.

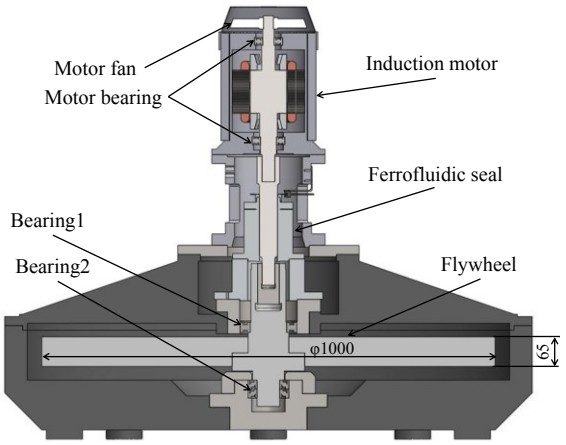

Fig. 1. Configuration of a proposed flywheel system that employs the general purpose motor and ball bearings.

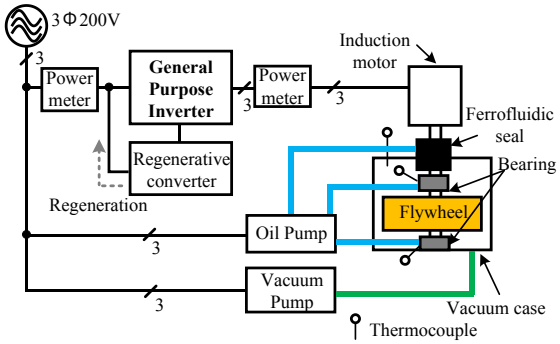

Fig. 2. Block diagram of the flywheel system including the measurement system and the auxiliary devices.

IV. Analysis Method of the Steady State Loss

In this section, the losses that occur in a steady rotation are separated into mechanical losses and electrical losses. From this analysis, the factors of the steady state loss that occur in the system will be clarified. Moreover, further efficiency of the flywheel system is considered.

A. Windage loss

The frictional losses that occur between the surface of the flywheel and the surrounding fluid are calculated by (1) from the shape of the flywheel and the friction moment.

$$P_w = C_{ms}\rho\omega^3(r_o^5 - r_i^5) + C_{mc}\rho\omega^3 r_o^2 r_i^2 t_i \quad \ldots (1)$$

where, C_{ms} is the moment coefficient of the friction of the top and bottom, C_{mc} is the moment coefficient of the friction of the side, ω is the angular velocity of the body revolution [rad/s], r_o is the radius of the vacuum case, r_i is the radius of the flywheel, t_i is the thickness of the rotational axis of the flywheel.

However, the friction moment fluctuates depending on the state of the fluid in the vacuum case. In this case, it is difficult to obtain a simple formula. Therefore, the windage loss is analyzed by using the computational fluid dynamics (CFD). Unstructured grid-based thermal fluid analysis system SCRYU / tetra (*software cradle*) is used for the analysis. In the model which faithfully reproduces the real system, the computation time increases the complexity of the analysis. Therefore, the simplified model eliminates extraneous parts and mechanisms are used for analysis. As an analysis condition, the fluid flow is turbulent and SST k-ω model is used as a model for turbulence. SST k-ω is a model that combines the k-ε model based on the k-ω model. In the vicinity of the wall, k-ω model's predictive accuracy is better separated flow is used. On the other hand, the k-ε model is used in an area away from the wall. As the initial condition, the pressure in the vacuum case is 500 Pa, the temperature is 10 degree Celsius. In addition, the fluid is rotated around the axis of the flywheel.

Fig. 4 shows the analysis of the ambient pressure of the flywheel. The analysis conditions are as follows: the steady rotational speed is 3315 r/min and the vacuum in the vacuum case is 500 Pa. From the analysis, the pressure increases toward the radial direction from the center of the flywheel. This is because an increasing in losses due to the friction of the fluid by increasing the peripheral speed.

B. Bearing loss

The bearing loss P_B is obtained by (2) from the rotational speed n and the friction moment of the bearing M.

$$P_B = 1.047 \times 10^{-4} nM \quad \text{.....(2)}$$

Additionally, the frictional moment can be separated into frictional moment M_o that depends on the load and the friction moment M_l that is independent from the load.

$$M = M_o + M_l \quad \text{.....(3)}$$

$$M_o = f_o \times 10^{-7} (un)^{2/3} {d_m}^3 \quad \text{.....(4)}$$

$$M_l = f_l P d_m \quad \text{.....(5)}$$

where, f_o is the coefficient that depends on the format and the method of the bearing lubrication, u is the viscosity of the lubricant, d_m is the inner diameter of the pitch of the rolling elements, f_l is the coefficient that depends on the magnitude and the direction of the load, P is the load on the bearing.

Table 2 shows the value used to calculate the bearing loss. In this system, two bearings are arranged at the bottom and one at the top of the flywheel. The bearing losses at each rotational speed are calculated by (4) and (5).

C. Copper loss with respect to the fundamental wave

In this section, the losses generated by the motor are separated into the copper loss and the iron loss.

Fig. 5 shows the equivalent circuit of the induction machine with respect to the fundamental wave. Table 3 shows the specifications of the motor that is used in the prototype system. From the equivalent circuit, the relationship between

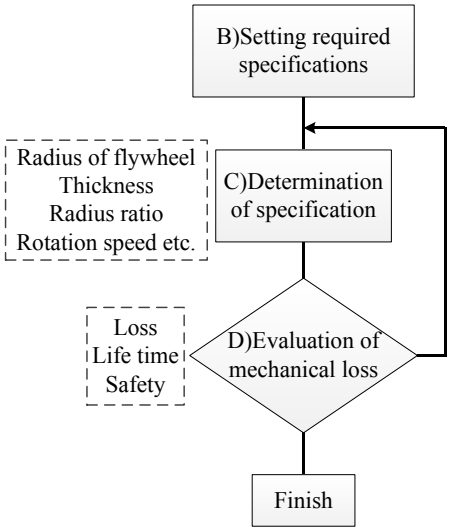

Fig. 3. Low-loss design algorithm of the flywheel with a focus on mechanical loss.

Table 1. Specifications of the flywheel which is calculated from the low loss design.

Flywheel	Material	SCM440
	Radius	500 mm
	Thickness	65 mm
	Weight of the Flywheel	392 kg
	Stored Energy	3.0 MJ at 3315 r/min
Motor/Generator	MLC1115C (*Fuji Electric*)	
Inverter	FRN 37G11S-2 (*Fuji Electric*)	

secondary input P_2 and the mechanical output P_{mec} is represented by (6).

$$P_2 : P_{mec} = 1 : (1 - s) \quad \text{.....(6)}$$

From this equation, the secondary resistance is calculated by (7).

$$R_2' = \frac{s}{1-s} \frac{1}{3} {I_2}'^2 \quad \text{.....(7)}$$

Note that the slip s is calculated from the actual speed and the synchronous speed of the induction motor. In addition, the secondary current I_2' is calculated from the no-load test of the motor itself. In the no-load test, the output resistance R_2'/s can be regarded as almost infinity because the slip s is almost zero. At this time, the current flowing through the circuit will be all the excitation current I_o. Therefore, the secondary current I_2' is calculated by (8).

$$I_2 = I_1 - I_o \quad \text{.....(8)}$$

From these results, the copper loss for the fundamental wave is expressed by (9).

$$P_c = 3R_1 {I_1}^2 + 3R_2' {I_2}'^2 \quad \text{.....(9)}$$

D. Copper loss for harmonic

In the driving of the motor by an inverter with pulse width modulation (PWM), the harmonic voltage is applied to the

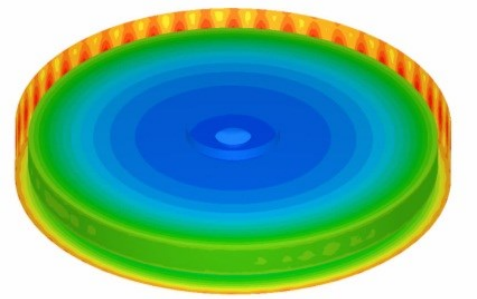

Fig. 4. Visualization of the ambient pressure of the flywheel at the rated energy storage.

Table 2. Condition for bearing loss calculation.

Bearing1	f_0	2
	f_l	0.0002
	Viscosity ν	17 mm^2/s
	Pitch diameter d_m	102.5 mm
	Rotation speed n	3315 r/min
	Load P	0 N
Bearing2	f_0	2
	f_l	0.00025
	Viscosity ν	17 mm^2/s
	Pitch diameter d_m	70 mm
	Rotation speed n	3315 r/min
	Load P	2528.4 N

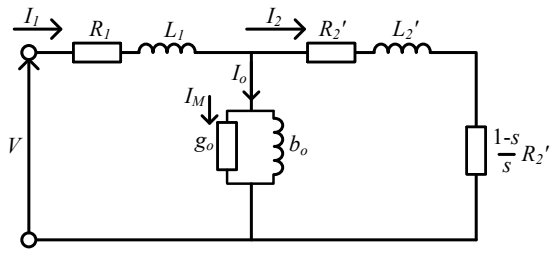

Fig. 5. Equivalent circuit of the induction machine with respect to the fundamental wave.

Table 3. Specifications of the motor that is used in the prototype system.

Rated Voltage	200V
Rated Current	14.4A
Output Power	3.7kW
Primary resistance R_1	1.01Ω
Excitation current I_o	5.90A

induction machine. As a result, the losses due to the harmonics occurs [8]. In this section, the copper loss caused by the harmonic component of the motor current is calculated.

Fig. 6 shows the analysis of the harmonic current at the rated energy storage. Note that the analysis results are normalized by the amplitude of the fundamental current. From the analysis, it is confirmed that the harmonic components due to the carrier frequency occurs. In the analysis of the copper loss with respect to the fundamental wave obtained in the preceding paragraph, the copper loss for the harmonic component is not considered. Therefore, it is necessary to calculate the copper loss of the induction machine for harmonics.

Fig. 7 shows the equivalent circuit of one phase of the induction machine for harmonic. The harmonics generated by PWM is sufficiently high frequency region for the fundamental component. Therefore, the exciting component of the equivalent circuit with respect to the fundamental wave is ignored. In addition, the mechanical output can be ignored because it can be regarded that the slip by the harmonic component is 1. For these reasons, the loss for the harmonic component is represented by (10).

$$P_n = 3(R_1 + R_2')I_n'^2 \quad \text{..... (10)}$$

E. Iron loss

From the equivalent circuit of the induction machine with respect to the fundamental wave, the iron loss is expressed by (11) by using the excitation conductance.

$$P_i = 3\frac{I_M{}^2}{g_o} \quad \text{.....(11)}$$

In addition, the excitation conductance g_o is expressed by (12).

$$g_O = \frac{P_o - W_m}{V_1{}^2} \quad \text{.....(12)}$$

where, P_o is input power at no load, W_m is the mechanical loss at no load.

V. EXPERIMENTAL RESULTS

A. Analysis of the steady state loss

Fig. 8 shows the measurement result of the steady state loss in experiment with prototype FESS as shown in Fig. 1. In this experiment, the rotation speed is 3315 r/min, the vacuum case is kept at 500 Pa. The mechanical loss and the electrical loss are separated by a free-run test at the beginning. Free-run test is a test for electrically disconnecting the inverter and the motor with the energy stored in the flywheel. In this state, the stored energy is consumed only by mechanical loss. Therefore, the mechanical loss is calculated from the time until the stored energy is consumed.

From the results, it is confirmed that the bearing loss accounts for 48.6% of all mechanical loss. Additionally, the electrical losses of the motor are accounted for 41.7% of the total loss. Therefore, it is necessary to improve the motor efficiency and reducing the bearing loss toward higher efficiency.

Fig. 9 shows the comparison of the experimental results with the results of a theoretical analysis of the mechanical loss. Note that P_m is the total value of the mechanical loss, P_f is the loss of the magnetic fluid seal, P_{em} is the mechanical loss of the motor. In addition, the loss of the seal and the motor mechanical loss are calculated from the free-run test.

From the Fig. 9, the analysis values agree with the experimental results. Therefore, it is confirmed that the

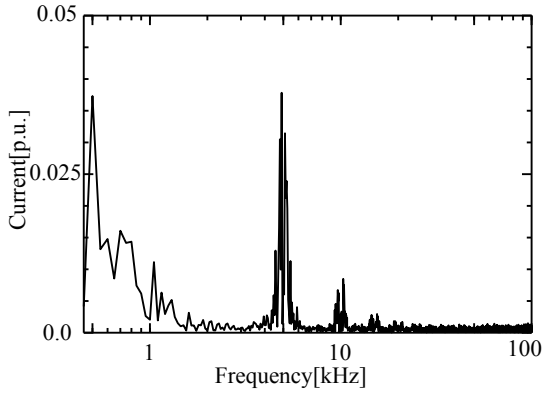

Fig. 6. Analysis of harmonic current at the rated energy storage. The analysis results are normalized by the amplitude of the fundamental current.

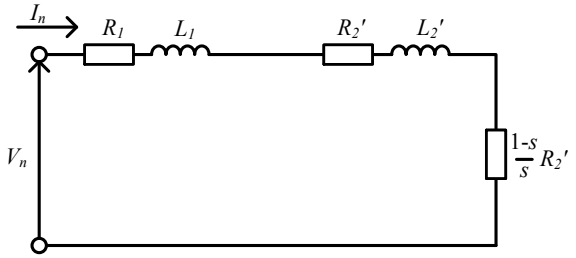

Fig. 7. Equivalent circuit of the induction machine for harmonic wave.

analytical method has high accuracy. Additionally, the value obtained by subtracting the copper loss of all electrical losses became 192 W. On the other hand, the theoretical calculation of the iron loss is 167 W. It is considered that the cause of the error is the use of a simple equivalent circuit. Therefore, it is necessary to use of the electromagnetic analysis in order to improve the accuracy of analysis of the iron loss.

B. Analysis of the energy storage efficiency

In this section, the energy storage efficiency of the prototype system is analyzed. This property is divided into a discharging efficiency and a charging efficiency. The charging efficiency is the ratio of the energy consumed for storing the desired energy. On the other hand, the discharging efficiency is the ratio of actual energy can be released with respect to stored energy.

Fig. 10 shows the experimental result of the energy storage, Fig. 11 shows the experimental result of the energy discharge. In the experiment of energy storage, the flywheel is accelerated from 2700 r/min to 3315 r/min. In the discharge test, the flywheel is decelerated from 3315 r/min to 2700 r/min.

The stored energy is calculated using (13) from the rotational angular velocity and the moment of inertia of the flywheel *J*.

$$E = \frac{1}{2} J\omega^2 \quad \text{.....(13)}$$

From this equation, it is calculated that the amount of the energy change is 1.01 MJ when the rotational speed changes from 2700 r/min to 3315 r/min.

Next, the energy storage efficiency is calculated using the experimental results. From the Fig. 10, the energy input in order to store the energy of 1.01 MJ is 1.34 MJ. Therefore, the charging efficiency is 75.4%. From the Fig. 11, it is confirmed that the energy is discharged 0.78 MJ. Therefore, the discharging efficiency is 77.2%.

The discharging efficiency of the energy storage devices is as follows: the lead acid battery is 75-85%, a redox flow battery is approximately 70%, an EDLC is approximately 90%. Therefore, it is confirmed that the energy storage efficiency of the prototype flywheel is about the same as the current main power storage device.

C. Evaluation of the cost

Table 4 shows the estimation of the cost of the proposed system. Note that the material of the flywheel is used chromium-molybdenum steel. Here, cost ratio of the material in flywheel is assumed as 1. On the other hand, cost ratio of the magnetic fluid seal and other components becomes 5.0 to be relative to the material cost of the flywheel. The most of this cost is accounted for the magnetic fluid seal. Therefore, it is necessary to consider the structure which can achieve a sufficient vacuum without the magnetic fluid seal. From the results, it is confirmed that the material cost of the flywheel in the proposed system is very cheap. However, the total cost of the entire system including the processing cost and the other components becomes very expensive. Therefore, it is possible to achieve a more reasonable system by improving the manufacturing method and structure.

Next, the cost of the proposed system is compared with other energy storage devices. The comparison condition is the same as the energy storage. From the reference [9], total cost of EDLC energy storage systems becomes approximately 25% higher as compared to the proposed flywheel system. Note that specification of the capacitor to be used is as follows: the rated voltage is 2.5 V, a capacitance is 2700 F, the cost per unit is $30. From these results, it is confirmed that the proposed system can achieve a lower cost than an EDLC energy storage system depending on the manufacturing cost. However, the reduction of processing cost and component cost are important issue for practical application of the flywheel.

VI. CONCLUSION

This paper introduced the performance of a power leveling system with a 3.0-MJ, 3315-r/min flywheel energy storage. In this proposed system, simplification of the system is achieved by applying the general purpose induction machine and the ball bearings. Additionally, the flywheel is designed with low loss design focused on the mechanical loss. From the loss analysis, it is confirmed that the bearing loss accounts for 48.6% of all mechanical loss. Moreover, the energy storage efficiency is measured by experiments. As a result, it is confirmed that the energy storage efficiency of the prototype flywheel is about the same as the current main power storage device. Towards higher efficiency, authors will consider the application and its low loss design of a permanent magnet motor and the pivot bearing. In the cost evaluation, it is

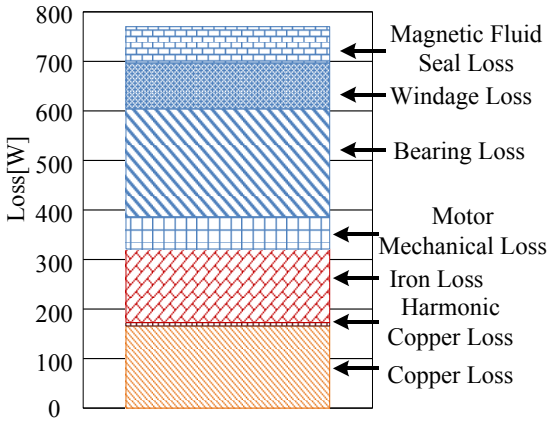

Fig. 8. Loss analysis results at the rated energy storage. In the experiment, the steady rotation speed is 3315 r/min and the pressure of the vacuum case is 500 Pa.

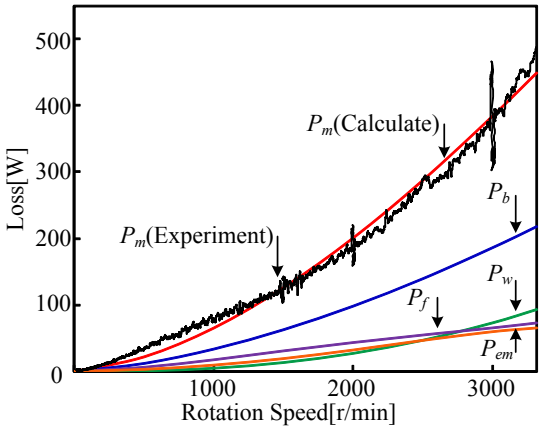

Fig. 9. Comparison of theoretical calculations and experimental results of mechanical loss.

Table 4. Estimation of the cost of the proposed system.

Components	Cost ratio
Material cost of Flywheel (SCM440)	1.0
Other material cost	5.5
Power converter	2.9
Induction machine	1.3
Ball bearings	2.6
Other components	5.0
Total cost	18.2

confirmed that the proposed system is fabricated approximately $8000 except for manufacturing cost. In future work, the optimal design method of the flywheel considering the processing cost and the component cost is established.

ACKNOWLEDGEMENT

A part of this study was supported by industrial technology grant program in 2011 from new energy and industrial technology development organization (NEDO) of Japan.

REFERENCES

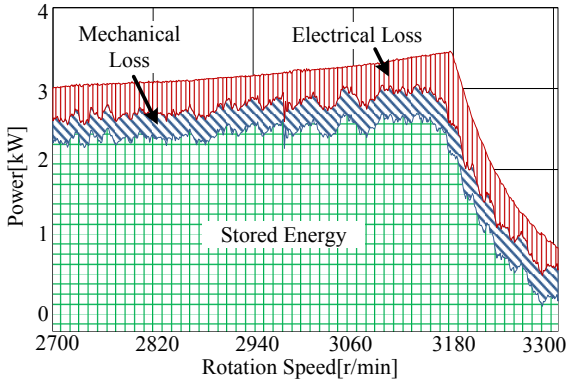

Fig. 10. Analysis of the efficiency of energy storage when the rotation speed of flywheel is increased from 2700 r/min to 3315 r/min.

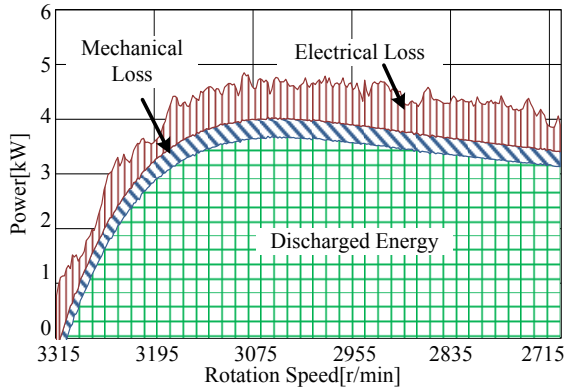

Fig. 11. Analysis of the efficiency of energy discharge when the rotation speed of flywheel is decreased from 3315 r/min to 2700 r/min.

[1] M.Uno, K.Tanaka," Accelerated Charge-Discharge Cycling Test and Cycle Life Prediction Model for Supercapacitors in Alternative Battery Applications" IEEE Trans on industrial electronics, Vol.60, No.6, pp.2131-2138(2013)

[2] B.H.Kenny, P.E.Kascak, R.Jansen, T.Dever, W.Santiago,"Control of a High-speed Flywheel System for Energy storage in Space Applications",IEEE Trans on industry applications, Vol. 41, No. 4, pp. 1029-1038(2005)

[3] Z.Kohari, Z.Nadudvari, L.Szlama, M.Keresztesi, I.Csaki,"Test Results of a Compact Disk-type Motor/Generator Unit with Superconducting Bearings for Flywheel Energy Storage Systems with Ultra-low Idling Losses",IEEE Trans on applied superconductivity, Vol. 21, No. 3, pp. 1497-1501(2011)

[4] K.Murakami,M.Komori,H.Mitsuda,"Flywheel Energy Storage System Using SMB and PMB",IEEE Trans on applied superconductivity, Vol. 17, No. 2, pp. 2146-2149(2007)

[5] K. Tanaka, Y. Ohnuma, T. Fujimori, J. Itoh, N. Yamada: "Loss Analysis of a Flywheel Energy Storage System for an Energy Cache Operation", SPC Ishikawa, SPC-11-006, MD-11-032(2011)

[6] K. Tanaka, J. Itoh, S. Matsuo, N. Yamada: "Regenerative Power Control Method of Flywheel Power Leveling System Using Smith Dead Time Compensation Method", IEEJ JIASC, No. 1-58(2012)

[7] N. Yamada, T. Fujimori, S. Wakashima,"Prediction of Mechanical Losees of Small-scale Flywheel Energy Storage System", Transactions of the Japan Society of Mechanical Engineers, Series B, Vol.78, No.789(2012)

[8] T. Ogura, J. Itoh: "Evaluation of Total Loss of Both an Inverter and Motor Depending on Modulation Strategies", SPC Hamamatsu, Spc-09-184, LD-09-074(2009)

[9] M. Ortuzar, J. Moreno, J. Dixon, "Ultracapacitor-based Auxiliary Energy System for an Electric Vehicle: Implementation and Evaluation", IEEE Trans on industrial electronics, Vol. 54, No. 4, pp.2147-2156(2007)